D. Covalency

The introduction of covalency ($\gamma>0$) tends to unpair the $2p\sigma$ electrons on the fluorine ions and to pair the hydrogen electron. Therefore the effect on the hyperfine constants is simply to reduce B and increase b. a is affected only through the normalization constant and, for small γ, does not change.

Table IV shows the effect of γ on the hyperfine constants in the Heitler–London model. If we assume that γ changes proportional to S as the shift of Δg with pressure implies,[13] then there is no effect on the pressure derivatives. We have chosen $\gamma=0.03$ to fit the measured g shift at room temperature.[13]

IV. CONCLUSIONS

It is possible to understand the values of the various hyperfine constants and their shifts with pressure and temperature on the basis of the simple Heitler-London model if local vibrational modes, lattice dilation and charge transfer are also considered. However, a more realistic calculation which solves the Hamiltonian for the complete many-electron system is clearly called for.

ACKNOWLEDGMENTS

This problem was suggested to the author by Professor G. B. Benedek, who contributed greatly with his interest and guidance both during the experiment and in the organization and presentation of this paper. The pressure bomb and microwave cavity as well as parts of the press were machined by A. Pukt who also made many valuable design suggestions. R. T. Schumacher kindly supplied the CaF_2 samples. The author is pleased to acknowledge helpful conversations with Professor Schumacher, Dr. J. L. Hall, and Dr. J. G. Castle, Jr.

PHYSICAL REVIEW VOLUME 161, NUMBER 2 10 SEPTEMBER 1967

Range Measurements in Oriented Tungsten Single Crystals (0.1–1.0 MeV). I. Electronic and Nuclear Stopping Powers*

L. ERIKSSON,† J. A. DAVIES,‡ AND P. JESPERSGAARD
Institute of Physics, University of Aarhus, Aarhus, Denmark
(Received 28 April 1967)

Range distributions of Na^{24}, P^{32}, K^{42}, Cr^{51}, Cu^{64}, Br^{82}, Kr^{85}, Rb^{86}, Sb^{122}, Xe^{125}, Xe^{133}, W^{187}, and Rn^{222} ions in the energy region 0.1–1.0 MeV have been measured in oriented tungsten single crystals by means of the electrochemical peeling technique. Wide-angle scattering of protons has, in some cases, been used to align the crystals to within $\pm 0.1°$. The range distrubutions consist of two peaks—a broad one at approximately the depth predicted for an amorphous target, and a sharp one at a much larger depth. The latter, caused by channeling, falls off very sharply on the more penetrating side. This well-defined paximum range has approximately an $E^{1/2}$ dependence, characteristic of electronic stopping. From range-energy relations, electronic-stopping cross sections are derived at a constant velocity of 1.5×10^8 cm/sec. The electronic stopping is roughly $\frac{1}{3}$ of that predicted for amorphous tungsten, but exhibits a strongly oscillating dependence on Z_1. These Z_1 oscillations are much larger than those reported previously in amorphous foils. Alto, the range dispersion between the ⟨100⟩ and ⟨110⟩ directions exhibits an oscillating Z_1 dependence. For perfectly channeled Xe ions along the ⟨100⟩ directions, electronic stopping is shown to dominate down to a few keV. The contributions from nuclear and electronic stopping become equal at about 4 keV, whereas the corresponding transition energy in amorphous tungsten would be ~2.5 MeV. The nuclear stopping contribution can be fitted theoretically by means of the momentum approximation down to ~0.5 keV. It is shown that, under certain conditions, range measurements in monocrystals provide information about amorphous ranges that is otherwise difficult to obtain. Good agreement between experiments and theoretical predictions is obtained. The present experiments also provide some information on the highly penetrating tail (supertail), earlier reported in tungsten. For comparison, a few range distributions have been measured in aluminum single crystals. The observed behavior is similar to that in tungsten, but the channeling is much less pronounced.

INTRODUCTION

SEVERAL years ago, computer studies[1–3] predicted that heavy ions of keV energies would penetrate to anomalously large depths along low-index crystallographic directions. Experimental evidence suggesting the existence of this channeling phenomenon came from range measurements in polycrystalline aluminum[4] and tungsten,[5] in which it was observed that a considerable fraction of the injected ions penetrated to larger depths than could be explained on the basis of randomly distributed target atoms. Measurements in amorphous anodic oxides,[5,6] on the other hand, showed no such penetrating component. Subsequently, the channeling

* A preliminary report of part of this work was presented at the Conference on Electromagnetic Isotope Separators and Related Ion Accelerators, and their Application to Physics, Aarhus, 1965 [Nucl. Instr. Methods **38**, 245 (1965)].

† Permanent address: Research Institute for Physics, Stockholm 50, Sweden.

‡ Permanent address: Chalk River Nuclear Laboratories, Research Chemistry Branch, Chalk River, Ontario, Canada.

[1] M. T. Robinson and O. S. Oen, Phys. Rev. **132**, 2385 (1963).

[2] M. T. Robinson and O. S. Oen, Appl. Phys. Letters **2**, 30 (1963).

[3] J. R. Beeler and D. G. Besco, J. Appl. Phys. **34**, 2873 (1963).

[4] J. A. Davies, F. Brown, and M. McCargo, Can. J. Phys. **41**, 829 (1963).

[5] M. McCargo, J. A. Davies, and F. Brown, Can. J. Phys. **41**, 1231 (1963).

[6] B. Domeij, F. Brown, J. A. Davies, and M. McCargo, Can. J. Phys. **42**, 1624 (1964).

effect on heavy ions was much more clearly demonstrated by range measurements in monocrystalline targets—aluminum,[7,8] tungsten,[9,10] copper,[11] and silicon.[12]

The paper by Kornelsen *et al.*[10] presented quantitative data on channeling in monocrystalline tungsten; it also showed the existence of a highly penetrating tail (supertail), containing about 0.1% of the injected ions. The influence of various parameters on these two effects was investigated. It was observed that, ignoring the tails, the channeled part of the distribution was characterized by a rather sharp fall-off, and that the *maximum range* introduced in this way approached an $E^{1/2}$ dependence at higher energies (see Fig. 7, Ref. 10). It was also seen that the channeled particles formed a "bump" on the most penetrating side of the distribution. In the case of 40-keV Ar^{41} in the ⟨111⟩ directions, this "bump" actually formed a small second peak in the distribution curve. These observations suggested that electronic effects play a dominant role in the stopping of channeled particles. Since the importance of nuclear stopping decreases with increasing energy, whereas the contribution from electronic stopping increases, it seemed worthwhile to extend the range-distribution studies in tungsten to higher energies. The present work therefore is an extension of the earlier experiments by Kornelsen *et al.* to higher energies, a greater variety of projectiles, and better crystal alignment. The main emphasis in the present paper (paper I) has been to measure electronic-stopping powers for channeled ions; a detailed study of the channeling mechanism is contained in paper II.[13]

By measuring maximum ranges at different energies, stopping powers for channeled atoms can be readily obtained. Electronic-stopping powers for various projectiles ($11<Z_1<86$) at constant velocity in different crystallographic directions are presented in Sec. 1.

By reinvestigating range data at low energies for Xe in tungsten,[10] it is possible to get information also about the nuclear stopping of a well-channeled ion. This analysis is presented in Sec. 2.

Section 3 contains some data on amorphous ranges in tungsten at higher energies, derived from the unchanneled peak in the range distributions.

The small, extremely penetrating supertail has not been the subject of the present investigation; in fact, its existence was more of an annoyance in some cases, as it tended to obscure the sharp fall-off of the channeled distribution. This tail was at first tentatively attributed to dynamic effects[10,14] ("superchanneling"), but later experiments[15] have shown the phenomenon to be of a three-dimensional diffusion character, probably an interstitial diffusion, starting after the channeled particles have come to rest. In the present work we have not specifically studied the supertail, but nevertheless some information about it is contained in our experiments. A short comment is given in Sec. 4.

A few range studies have also been performed in monocrystalline aluminum for comparison with tungsten. The results are contained in Sec. 5.

EXPERIMENTAL TECHNIQUE

A. General

The experimental technique is almost identical to that used in the earlier range measurements in tungsten. Briefly, a tungsten monocrystal was bombarded along a known crystallographic direction with a beam of monoenergetic radioactive ions. The activity of the crystal was measured, and then successive homogeneous layers of tungsten of known and reproducible thickness were removed from the crystal by anodic oxidation followed by chemical dissolution of the oxide (the method is described in Refs. 5 and 10). After each anodizing-stripping procedure, the residual target activity was measured. When normalized and plotted against the total thickness removed, this provides an integral range distribution of the radioactive atoms in the crystal. By differentiating this curve, one can also obtain the actual concentration profile of the embedded atoms.

B. Bombarding Facilities and Conditions

The crystals were mounted in the target chamber of the 600-keV heavy ion accelerator at Aarhus.[16] This accelerator is furnished with a universal ion source and the acceleration stage is followed by a 75° sector magnet. Energies greater than 500 keV were obtained by using doubly and, in the case of xenon, triply charged beams. For energies less than 100 keV, the Aarhus isotope separator[17] was utilized. The bombardment dose generally did not exceed 10^{13} atoms/cm^2.

Tungsten is known to have only a thin oxide coating (~10 Å) on its surface under normal conditions. Even so, at lower energies (<20 keV) an ultrahigh-vacuum technique had to be used in order to get meaningful range measurements.[10] At the higher energies used here, however, normal vacuum conditions were considered sufficient.

---

[7] G. R. Piercy, F. Brown, J. A. Davies, and M. McCargo, Phys. Rev. Letters **10**, 399 (1963).
[8] G. R. Piercy, M. McCargo, F. Brown, and J. A. Davies, Can. J. Phys. **42**, 1116 (1964).
[9] B. Domeij, F. Brown, J. A. Davies, G. R. Piercy, and E. V. Kornelsen, Phys. Rev. Letters **12**, 363 (1964).
[10] E. V. Kornelsen, F. Brown, J. A. Davies, B. Domeij, and G. R. Piercy, Phys. Rev. **136**, 849 (1964).
[11] H. Lutz and R. Sizmann, Phys. Letters **5**, 113 (1963).
[12] J. A. Davies, G. C. Ball, F. Brown, and B. Domeij, Can. J. Phys. **42**, 1070 (1964).
[13] L. Eriksson, following paper, Phys. Rev. **161**, 235 (1967). Referred to as paper II.
[14] C. Erginsoy, Phys. Rev. Letters **12**, 366 (1964).
[15] J. A. Davies and P. Jespersgaard, Can. J. Phys. **44**, 1631 (1966).
[16] E. Bøgh, P. Dahl, H. E. Jørgensen, and K. O. Nielsen, Institute of Physics, University of Aarhus, Denmark, Report, 1965 (unpublished).
[17] K. O. Nielsen and V. Toft, Institute of Physics, University of Aarhus, Denmark, Report, 1965 (unpublished).

TABLE I. Description of the selective counting experiments.

Isotopes injected	$T_{1/2}$	Main decay	Detection	k factors
Kr^{85}	10.6 yr	99% 0.672-MeV β^-→ground state of stable Rb^{85}	β	$(0.47\pm0.04)\times10^{-3}$
Br^{82}	36 h	100% 0.444-MeV β^-→excited state in stable Kr^{82}	γ	7.04 ± 0.07
Kr^{85}	10.6 yr	see above	β	0.0124 ± 0.0006
Rb^{86}	19 d	91% 1.777-MeV β^-, 9% 0.696-MeV β^-→stable Sr^{86}	β (with absorber)	4.33 ± 0.15
Xe^{125}	18 h	100% ϵ→excited states in 60d I^{125} (strong 0.243-MeV γ, 0.188-MeV γ, ···).	γ (excess, lower level)	0.105 ± 0.001
Xe^{133}	5.3 d	99% 0.347-MeV β^-→99% 0.081-MeV γ in stable Cs^{133}	γ (channel)	0.0108 ± 0.0004

C. Orientation of Crystals

In all the earlier range studies, the crystals were oriented by x-ray diffraction methods, with an angular uncertainty of at least ±1°. In the present work, since a high degree of angular orientation was often desirable, we have used wide-angle scattering of protons to align the crystals to within 0.1° of any desired orientation. (This simple orientation technique is described in Ref. 18.) After such an alignment, the crystal was bombarded *in situ* with the desired radiotracer via the same collimating system.

The integrated proton dose never exceeded 10 μC, and hence should not introduce an appreciable amount of hydrogen or of radiation damage into the lattice. To prevent significant amounts of hydrogen accumulating from successive runs on the same crystal, a layer of tungsten somewhat greater than the range of the 400-keV protons used (viz. ~4 mg/cm²) was periodically etched away.

At these higher energies, we find that the actual range distribution is very sensitive even to small misorientations. Figure 4, Ref. 19, for example, shows how even a 0.88° misorientation from the ⟨100⟩ direction drastically changes the integral range distribution of 500-keV Xe ions. Further experiments have shown that, in order to obtain quantitatively significant channeling distributions of heavy ions, the desired crystal axis must be aligned with the ion beam to within one or two tenths of a degree. In previous channeling studies, this condition was not usually fulfilled.

D. Projectiles and Crystals

Different radioactive ions (Na^{24}, P^{32}, K^{42}, Cr^{51}, Cu^{64}, Br^{82}, Kr^{85}, Rb^{86}, Sb^{122}, Xe^{125}, Xe^{133}, W^{187}, and Rn^{222}) have been injected along the ⟨100⟩ and ⟨110⟩ directions of tungsten crystals and, in a few cases, along the ⟨111⟩ directions and the {110} planes. Three different crystals, cut respectively with the ⟨100⟩, ⟨110⟩, and ⟨111⟩ directions close to the surface normal, have been used in all the experiments. These crystals were described in Ref. 10.

[18] J. U. Andersen, J. A. Davies, K. O. Nielsen, and S. L. Andersen, Nucl. Instr. Methods **38**, 210 (1965).

[19] J. A. Davies, L. Eriksson, and P. Jespersgaard, Nucl. Instr. Methods **38**, 245 (1965).

E. Counting

The activity was normally followed down to 10^{-3}–10^{-4} of the initial counting rate, which was ~10^5 counts/min.

Most of the radiotracers used were β emitters; a 2π flow-type proportional β counter (dead time ~5×10^{-6} sec) has been used as detector because of its high efficiency and low background. For the penetration depths involved in these range studies (1–6 mg/cm²), the scattering and absorption contributions to the observed β counting rate are constant to within ±3% in most cases, and could therefore be neglected. In the case of γ emitters, a NaI crystal was used.

F. Isotope Selective Counting

In order to determine accurately the small differences in maximum range between neighboring heavy elements (Br–Kr and Kr–Rb), pairs of range distributions have been measured simultaneously. To do this, the two radioisotopes were injected into the crystal in successive bombardments, and then the individual range distributions were measured simultaneously by isotope selective counting. Both bombardments were carried out with the same alighment and beam energy. Since in these experiments we had to use a somewhat larger dose than usual, the bombardments were normally carried out in several stages (e.g., Br^{82}–Kr^{85}–Br^{82}–Kr^{85}–Br^{82}) in order to average out any small dose effect that might occur. The same technique has also been used in studying the effect of misalignment (Fig. 4, Ref. 19) in which Xe^{125} and Xe^{133} ions were alternatively injected at different angles, and also to show the nonexistence of an isotope effect.

Table I summarizes how our selective counting has been performed. The k factors are obtained by counting pure test samples in polycrystalline foils; they give the fractional counting rate of each isotope in the channel set for the other isotope. This enables the two distributions to be deduced accurately from the observed data. Previously, Ball and Brown[20] have used selective counting to obtain simultaneously Xe^{133} and Cs^{134} distributions in tungsten at 40–125 keV. As pointed

[20] G. C. Ball and F. Brown, Can. J. Phys. **43**, 676 (1965).

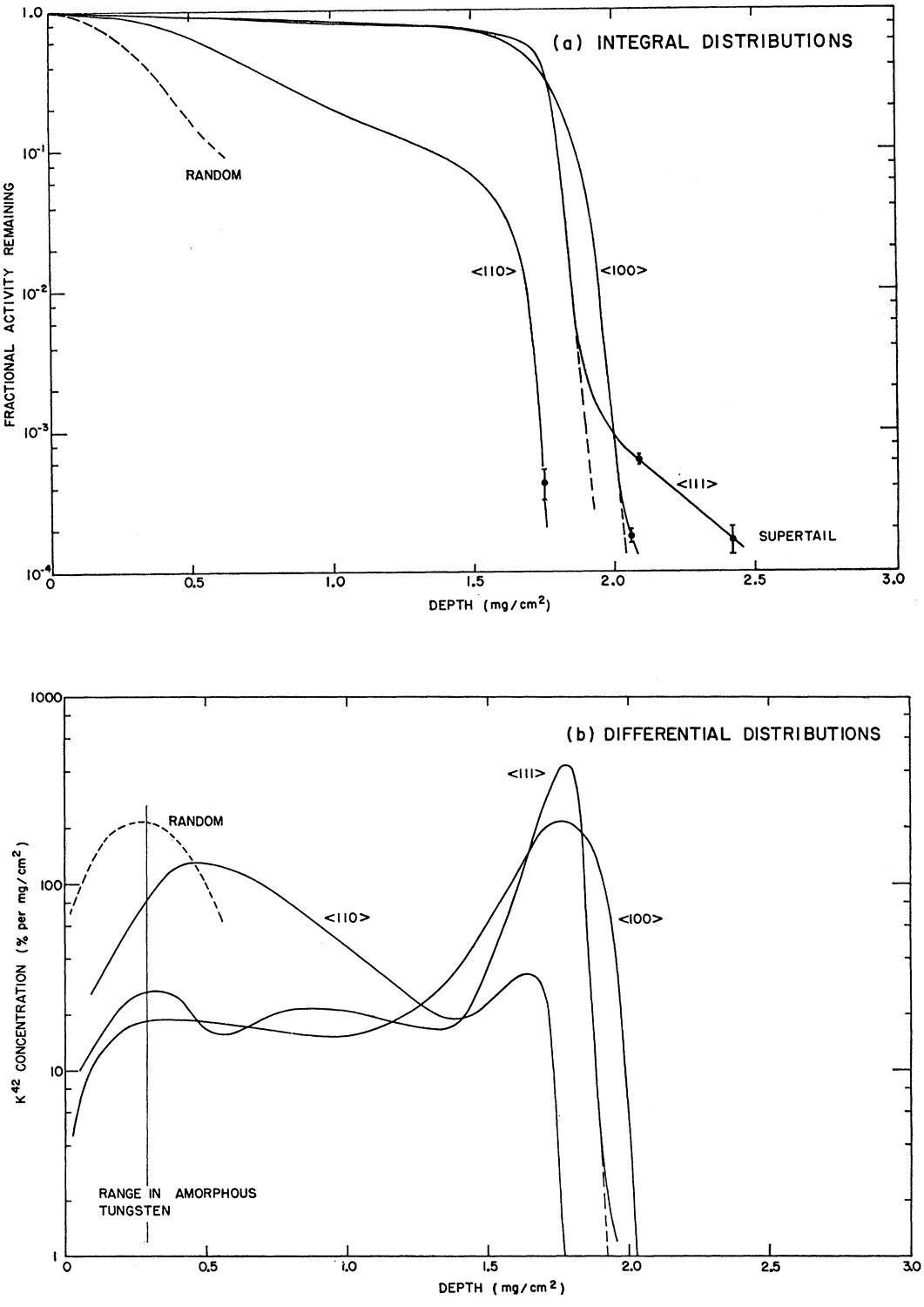

FIG. 1. Range distributions of 500-keV K^{42} ions along the ⟨100⟩, ⟨111⟩, and ⟨110⟩ directions in tungsten: (a) integral distributions; (b) differential distributions. The crystal has been aligned to $\pm 0.1°$ by wide-angle scattering of protons. Statistical errors become significant only near the end of the integral distributions. For the main part of these distributions, statistical errors fall within the width of the curve, and experimental points have therefore been omitted.

out by them, the fact that the range distributions fall off rapidly near the maximum range means that even a 5% difference in maximum range will cause one of the radiotracers to completely disappear, while a significant amount of the other one is still present (see, for example, Fig. 6).

1. ELECTRONIC STOPPING OF CHANNELED IONS

A. Stopping Mechanisms

Two processes are responsible for the stopping of a slow heavy ion: elastic encounters with atoms as a whole (nuclear collisions), and inelastic encounters in which energy is transferred to electrons as excitation and ionization energy (electronic collisions). Normally, these two processes are treated as uncorrelated.[21–23]

Ordinarily, for a given projectile and target, the energy alone determines which stopping process predominates; however, in a single crystal, as will be seen, the trajectory of the particle can be equally important.

At sufficiently high energies, the loss to atomic electrons always predominates, and the Bethe-Bloch formula applies. The stopping cross section increases with decreasing energy and reaches a maximum at a velocity of the order of $v_1 = v_0 \times Z_1^{2/3}$, where v_0 is the Bohr velocity and Z_1 the atomic number of the incoming particle. For potassium and xenon beams, v_1 corresponds to energies of about 50 and 650 MeV, respectively. In the velocity range $0 < v < v_1$ (i.e., in all the cases studied here), the electronic stopping should be roughly proportional to velocity.[23,24] Nuclear stopping,[23] on the other hand, exhibits a maximum at very much lower energies, and then decreases with increasing energy. In amorphous tungsten the energy at which the electronic and nuclear stopping should be equal is 0.24 MeV for potassium and 2.7 MeV for xenon. Below these values, one ordinarily cannot measure the electronic stopping because of the large nuclear-stopping contribution. In a single crystal, however, the nuclear stopping encountered by a perfectly channeled atom is so much suppressed that electronic stopping can be the dominant process down to much lower energies.

B. Evidence of Electronic Stopping

Figure 1 shows integral and differential range distributions of 500 keV K^{42} ions along the ⟨100⟩, ⟨111⟩, and ⟨110⟩ axes. Unlike the lower-energy results, each differential distribution consists of two distinct peaks. The one closer to the surface occurs at approximately the depth predicted for amorphous tungsten, and presumably corresponds to particles that are scattered out of the aligned beam as they enter the crystal. This scattering may arise partly from various imperfections such as a surface oxide layer; however, even in a perfect lattice, a significant part of the beam will enter the crystal close enough to an atomic row to be immediately deflected out of the aligned low-index direction. Such particles undergo normal stopping (which at these energies would be mainly due to elastic nuclear collisions). The channeled particles forming the second peak have evidently maintained their alignment with the low-index direction throughout most of their path in the crystal; hence, they experience a lower rate of energy loss and a correspondingly larger range.

TABLE II. R_{max} values in monocrystalline tungsten. Typical errors 5%.

Ion	Energy (keV)	Maximum range (mg/cm²) ⟨100⟩	⟨110⟩
Na^{24}	40	1.35[a]	...
	80	1.95	1.35
	150	3.00	2.10
	200	2.75	2.30–2.50
	300	3.80	...
	400	4.30	3.20
	500	4.70	3.60
P^{32}	300	2.30–2.40	2.05
	500	3.30	2.75
K^{42}	40	0.47	0.39
	70	0.67	...
	150	1.07	0.95
	300	1.53	1.33
	500	2.02[b]	1.75[b]
	900	2.70	...
Cr^{51}	70	0.64	0.50–0.56
	150	1.02	0.83
	200	1.48	1.03
	300	...	1.30
	400	1.83[b]	1.60
	500	2.02[b]	1.90
Cu^{64}	200	3.6–3.8	2.8
	400	5.2	4.2
	500	5.8[b]	4.5[b]
Kr^{85}	20	0.41[a]	0.25[a]
	40	0.64[a]	...
	200	1.95	1.65
	450	3.13	2.80
	900	4.70	4.15
Sb^{122}	250	4.15	2.20
	500	6.40	3.45
	1000	8.60	5.20
Xe^{133}	20	0.39[a]	0.22[a]
	40	0.70[a]	0.41[a]
	80	1.13[a]	0.76[a]
	160	1.90[a]	1.28
	400	3.10	2.20
	500	3.60	2.70
	1500	6.40	4.50
W^{187}	50	0.63	...
Rn^{222}	100	1.6	...

[a] From Ref. 10.
[b] Mean value

[21] N. Bohr, Kgl. Danske Videnskab. Selskab, Mat.-Fys. Medd. **18**, No. 8 (1948).
[22] J. Lindhard and M. Scharff, Phys. Rev. **124**, 128 (1961).
[23] J. Lindhard, M. Scharff, and H. E. Schiøtt, Kgl. Danske Videnskab. Selskab, Mat.-Fys. Medd. **33**, No. 14 (1963).
[24] O. B. Firsov, Zh. Eksperim. i Teor. Fiz. **36**, 1517 (1959) [English transl.: Soviet Phys.—JETP **9**, 1076 (1959)].

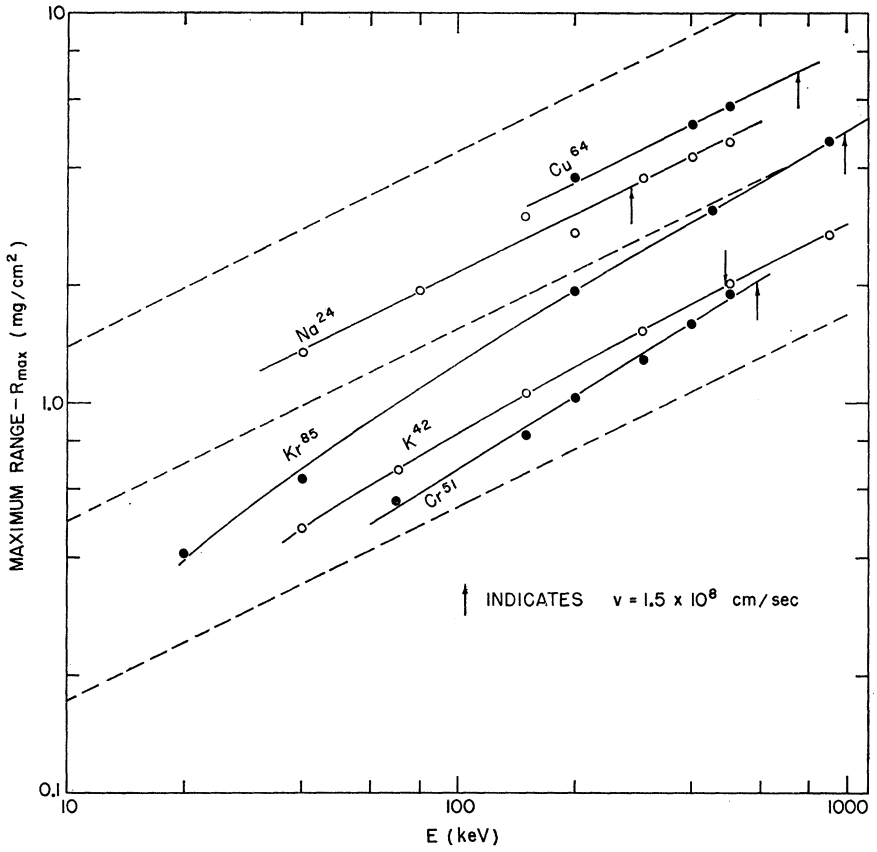

FIG. 2. R_{max}-versus-energy curves in tungsten along the ⟨100⟩ direction (for Cr^{51}, the ⟨110⟩ direction is shown). The arrows indicate the energy corresponding to $v=1.5\times10^8$ cm/sec. Dotted lines depict an $E^{1/2}$ dependence characteristic of electronic stopping.

Nuclear stopping depends strongly on the impact parameter, and therefore would give channeled atoms a rather broad range distribution: For example, a perfectly channeled atom would have a much longer range than one oscillating around the midchannel axis. Electronic stopping, on the other hand, is expected to vary only slowly over the central region of a channel and hence all channeled particles would have similar ranges. Consequently, the occurrence of a rather sharp peak indicates that, for the channeled atoms, electronic stopping is the dominant mechanism of energy loss.

In our experiments, channeled particles penetrate several thousand atomic layers before they are stopped. Some particles, therefore, start with a channeled trajectory but, because of scattering effects (impurities, defects, thermal vibrations, etc.), they are subsequently

TABLE III. Experimental values of S_e and p at $v=1.5\times10^8$ cm/sec.

Ion	E(keV)	S_e [10^{-14} eV cm^2/atom] ⟨100⟩	⟨110⟩	p ⟨100⟩	⟨110⟩
Na^{24}	280	4.8±0.3	6.5±0.4	0.50±0.05	0.50±0.05
P^{32}	370	6.4±0.4	7.8±0.4	0.38±0.08	0.40±0.05
K^{42}	490	15.0±0.6	17.3±0.9	0.48±0.03	0.50±0.03
Cr^{51}	590	14.2±0.9	13.9±0.8	0.42±0.03	0.35±0.05
Cu^{64}	750	6.4±0.7	8.1±0.8	0.50±0.05	0.50±0.05
Br^{82}	960	8.9[a]	11.1[a]		
Kr^{85}	990	10.2±0.5	13.2±1.3	0.40±0.05	0.45±0.05
Rb^{86}	1000	11.7[a]	15.2[a]		
Sb^{122}	1420	8.6±0.8	13.7±1.0	0.52±0.03	0.45±0.05
Xe^{133}	1550	14.0±0.7	20.5±1.0	0.50±0.05	0.50±0.05
Cs^{134}	1560	16.5[a]	24.2[a]		
Rn^{222}	2580	11 ±3			

[a] Measurements by the isotope selective counting technique.

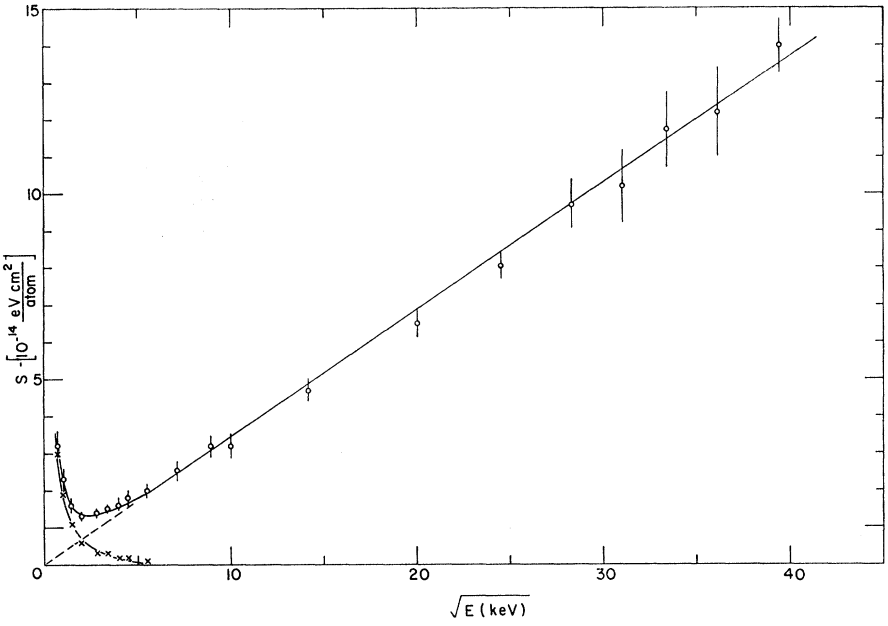

FIG. 3. Experimentally derived values of the total stopping cross section (open circles) versus energy for perfectly channeled Xe ions along the ⟨100⟩ direction in tungsten (below 100 keV, range data are from Ref. 10). The dotted line is an extrapolation of the electronic contribution to lower energies. Crosses indicate the nuclear stopping obtained by subtracting the extrapolated electronic stopping from the measured total values.

scattered out of the channeled beam. These particles contribute to the region between the first and the second peaks. If the fraction dechanneled is large, as for the poorer ⟨110⟩ direction, the first or "random" peak is not clearly resolved [see Fig. 1(b)]. Occasionally, a small third peak is observed in the range distribution [e.g., the ⟨111⟩ curve in Fig. 1(b)]; its significance is not clear.

A more direct confirmation that electronic effects dominate the stopping of channeled particles is ob-

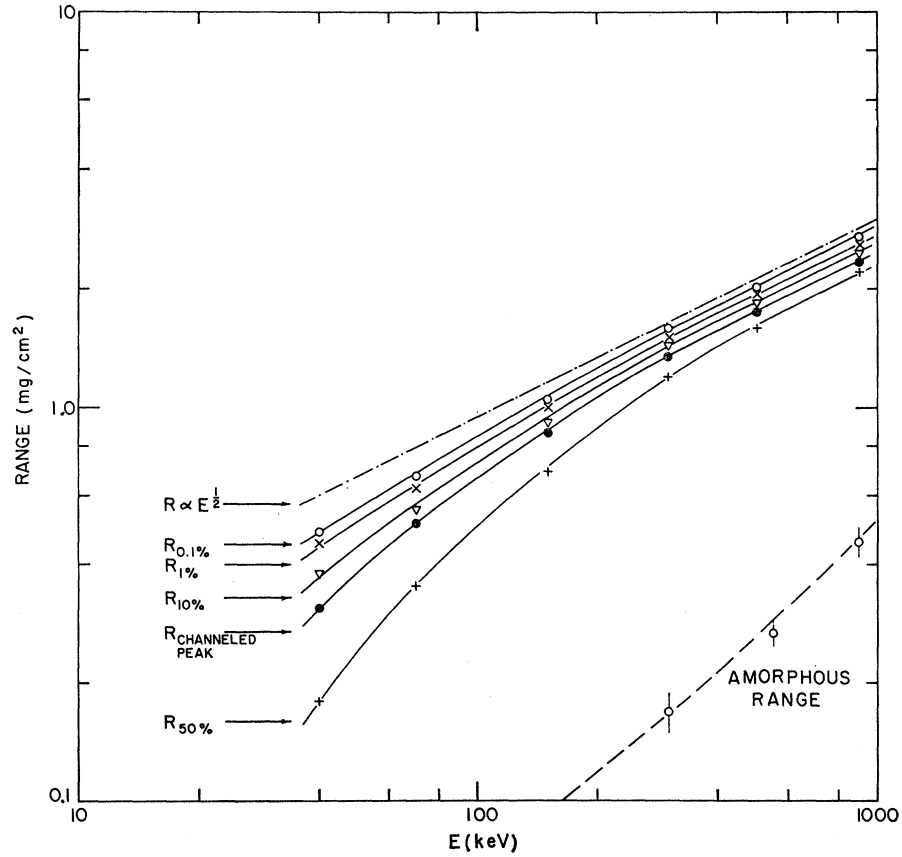

FIG. 4. Ranges versus energy for K^{42} ions along the ⟨100⟩ direction in tungsten. R_x (where x is in percent) is defined as the depth beyond which $x\%$ of the injected ions penetrate. For K^{42}, $R_{0.1}$ is a good approximation to the maximum range R_{max} [see Fig. 1(a)]. The most probable range of the channeled peak is also shown. For comparison, experimental values of the projected amorphous range have been included (see Sec. 3).

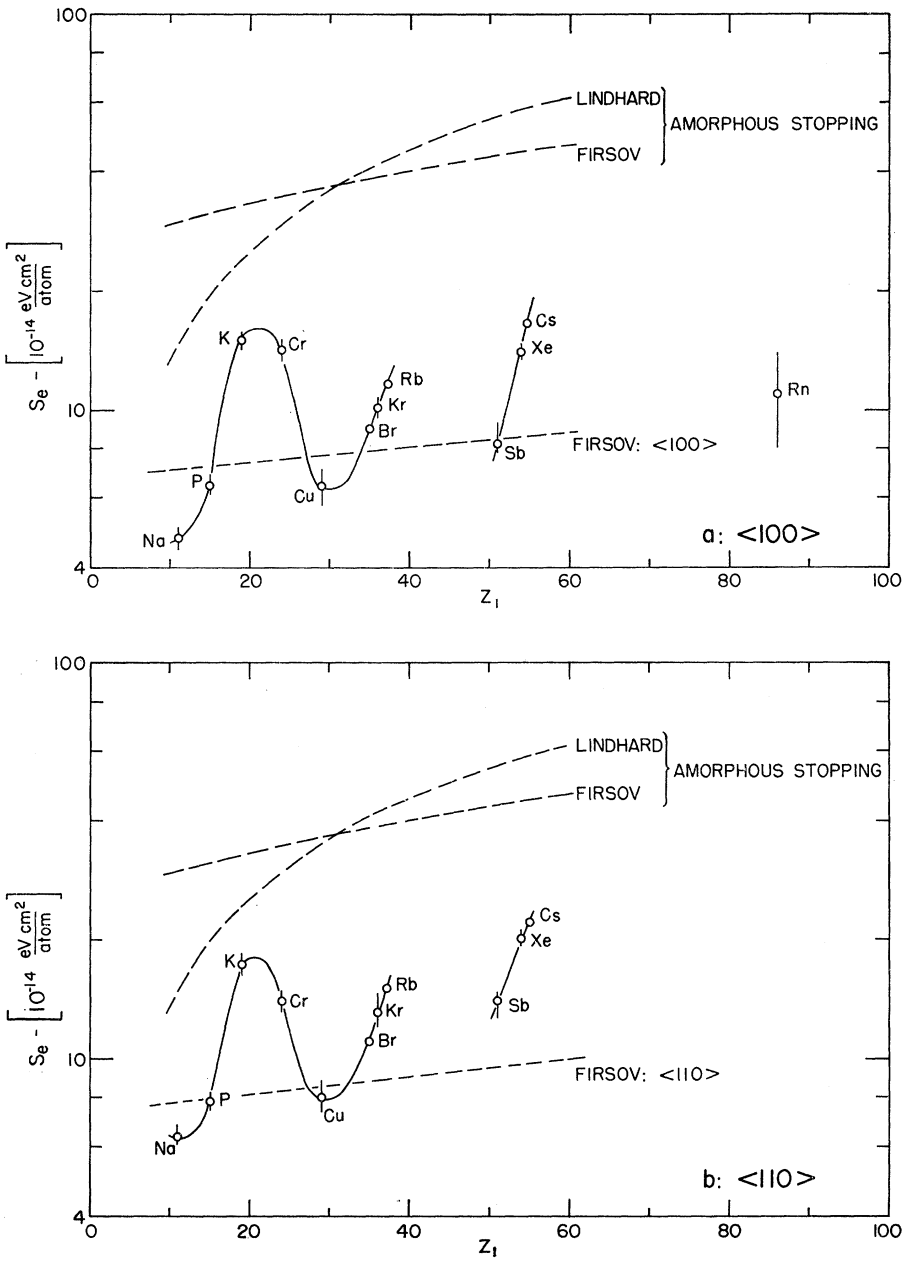

FIG. 5. Electronic-stopping cross sections (measured at a constant velocity $v=1.5\times10^8$ cm/sec) versus the atomic number of the projectile: (a) for the ⟨100⟩, and (b) for the ⟨110⟩ directions. Dotted lines give the Lindhard (Ref. 23) and the Firsov (Ref. 24) predictions for amorphous tungsten, and the prediction by Firsov (Ref. 24) for a perfectly channeled particle. The cross sections for Br and Rb are determined relative to Kr by selective counting techniques. The values for Cs are derived from Ref. 20.

tained by studying the energy dependence of the most penetrating part of the incident beam. As can be seen in Fig. 1, the measured distributions all have a very sharp cutoff and we therefore introduce the concept of a maximum range R_{max}. It seems reasonable to associate R_{max} with the range of the most *perfectly* channeled part of the incident beam. As is shown in Ref. 13, R_{max} is a rather useful experimental parameter—its value is almost independent of the surface oxide thickness, of damage effects, of slight misorientation, and even of lattice temperature. On the other hand, the *number* of particles approaching this maximum depth is found to be quite sensitive to all these factors. (Note that the supertail mentioned earlier has been disregarded in the present discussion.)

A preliminary study of the energy dependence of R_{max} (measured at 0.1% residual activity) for Xe in tungsten was given in Ref. 19, Fig. 2. Similar measurements have now been made for a series of other projectiles (Table II) and a few typical cases are illustrated in Fig. 2. In all cases, an approximate $E^{1/2}$ dependence, characteristic of electronic stopping, is observed. This can be seen more clearly in Fig. 3 in which the total stopping cross section S, derived by differentiating the R_{max}-versus-E curve, is plotted as a function of $E^{1/2}$. One finds that the linear relationship for electronic

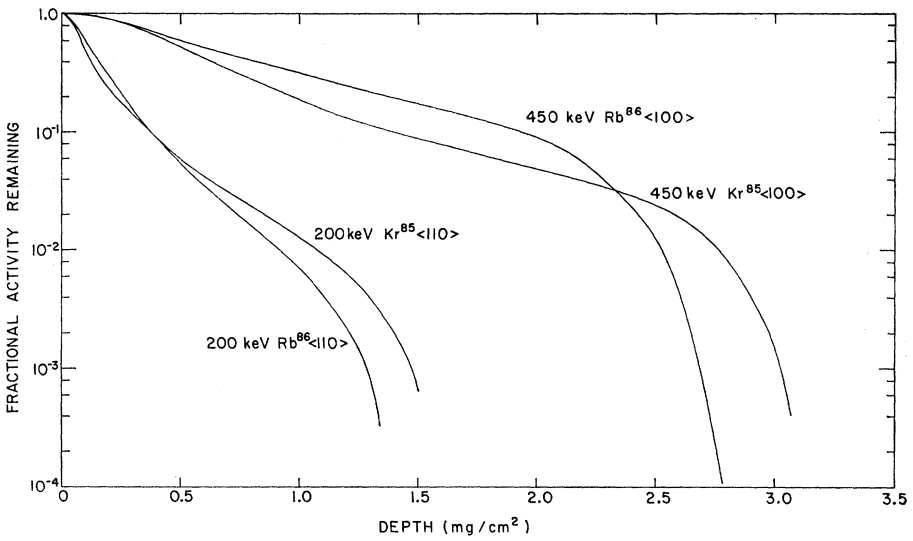

FIG. 6. Integral range distributions of 200- and 450-keV Kr^{85} and Rb^{86} ions along the ⟨100⟩ and ⟨110⟩ directions in tungsten, obtained by isotope selective counting.

stopping[23,24] is in fact maintained down to extremely low energies. The nuclear-stopping contribution (obtained by extrapolating this linear region, and then subtracting it from the total measured stopping) does not predominate until $E<4$ keV. In *amorphous* tungsten, on the other hand, the transition to nuclear stopping occurs at much higher energies, viz. around 2.7 MeV for Xe. Hence, the channeling process enables electronic stopping to be studied in an energy region where normally it would be completely masked by the nuclear stopping.

A more detailed discussion of the *nuclear* stopping contribution is contained in Sec. 2.

At this stage, it is perhaps important to point out that, because the integral range curve falls off so sharply, these derived stopping cross sections are relatively insensitive to the experimental method of defining R_{max}. Figure 4 shows the energy dependence of various types of range for K^{42} ions injected along the ⟨100⟩ direction. In this case, it is evident that even the median (i.e., 50%) range has almost an $E^{1/2}$ dependence. Furthermore, it can be seen that the vertical displacement between the curves is very small. Consequently, the derivation of the electronic stopping power does not depend appreciably on how R_{max} is defined.

TABLE IV. Maximum ranges of Br^{82} and Rb^{86} relative to Kr^{85}.

Ion	E(keV)	Range increase relative to Kr^{85} [a] ⟨100⟩	⟨110⟩
Br^{85}	200	+13.6%	···
	450	+13.8%	+17%±3%
Rb^{86}	200	−13.7%	−12.2%
	450	−12.2%	−12.7%

[a] Maximum ranges for Kr^{85} are given in Table II.

C. Electronic Stopping Powers

By differentiation of an R_{max}-versus-E curve the stopping power, $S=(1/N)\Delta E/\Delta R$, for the *perfectly channeled* beam is obtained. Since, as discussed above, the nuclear-stopping contribution is negligible, S can be directly equated to the electronic stopping S_e of a channeled atom.

In comparing cross sections for various channeled projectiles, it is convenient to keep the velocity v constant, as the electronic stopping should be approximately proportional to the velocity. For this purpose we have chosen $v=1.5\times10^8$ cm/sec, corresponding to $v/v_0=0.69$. Figure 5 compares the results for various projectiles along the ⟨100⟩ and ⟨110⟩ directions, and includes also the theoretical predictions applicable to a random stopping medium,[23,24] and to a perfectly channeled atom.[24] Table III lists the energies corresponding to our choice of v and the measured values of S_e.

In most cases, the measured range–energy curve overlaps the value corresponding to $v=1.5\times10^8$ cm/sec. Slight extrapolation has been necessary for Cr^{51}, Cu^{64}, and Sb^{122}. In the case of Rn^{222}, a much longer extrapolation was required and hence its error bar in Fig. 5 is much larger. The data for Br and Rb have been determined relative to Kr with considerable accuracy, using the selective counting procedure described in the previous section on experimental technique. Table IV summarizes the results of these experiments, and Fig. 6 shows a set of typical range curves.

The values for Cs in Fig. 5 are deduced from the work of Ball and Brown.[20] In measurements at 40 and 125 keV, they observed that R_{max} is 15–20% smaller for Cs than for Xe. Assuming that the same range–energy relation holds for both elements, this would indicate a 15–20% higher electronic stopping power for Cs—as shown in Fig. 5.

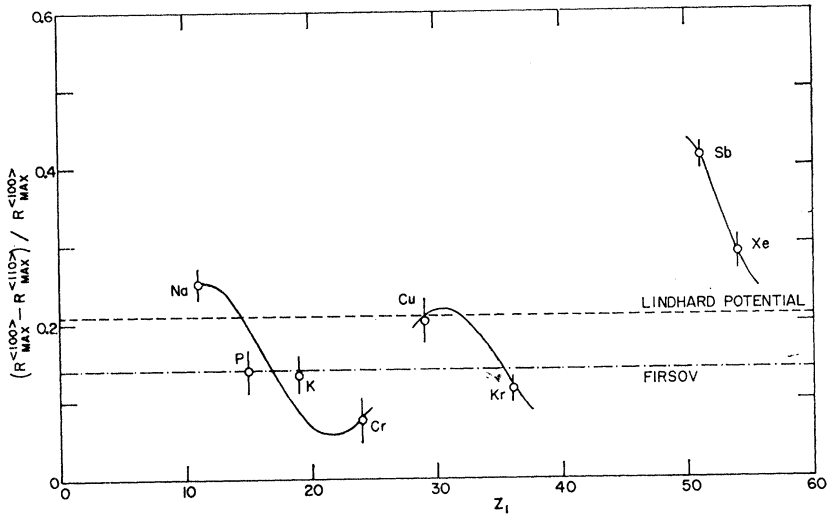

FIG. 7. Relative difference in maximum range along the ⟨100⟩ and ⟨110⟩ directions in tungsten as a function of the atomic number of the projectile. Also included are the predictions by Firsov (Ref. 24) and an estimate based on the mean electron density $\bar{\rho}$ along the mid-channel axes [calculated from Lindhard's "standard potential" (Ref. 30)], assuming the range is inversely proportional to $\bar{\rho}$.

It is tempting at these higher energies to draw a straight line through the experimental points (Fig. 2), and thus fit the stopping powers to an equation of the form $S_e \propto E^p$. According to theory, p should be around 0.5; the values obtained in the present work (Table III) are mostly within experimental error of this predicted energy exponent.

D. Discussion of Electronic Stopping Powers

Two main features in the above results should be noted:

(i) The observed S_e values (Fig. 5) are roughly one-third of the predicted values for amorphous tungsten.

(ii) The data cannot be fitted quantitatively to the existing theories[23,24] by a simple scaling factor, but oscillate around a "mean curve" by as much as 50%.

Lindhard's theoretical prediction of the electronic stopping power fits the experimental data in amorphous foils[25–29] reasonably well, but gives much higher values than those observed here for channeled atoms. The observed reduction in the electronic stopping power for the channeled beam is presumably due to the decreased electron density it encounters. Using Lindhard's potential,[30] the electron density $\bar{\rho}$ along the middle of the tungsten ⟨100⟩ channel is estimated[31] to be about $\frac{1}{20}$ of the mean electron density; the observed decrease in S_e is only about $\frac{1}{3}$. Of course, the electronic-stopping power is not expected to be exactly proportional to $\bar{\rho}$. Furthermore, the trajectory of even the most perfectly channeled ion may oscillate somewhat around the mid-channel axis, and this would tend to increase the mean electron density encountered by the channeled particle. Also, in Lindhard's treatment of the electron density, specific effects such as conduction electrons are not taken into account. In the case of tungsten, the large number of such electrons might increase considerably the electron density along the mid-channel axis. It is interesting to note that recent low-temperature measurements in gold[32] indicate that the maximum range of 40-keV Xe along the best channeling direction (the ⟨110⟩) is at least twice the value observed in tungsten along a comparable direction (either the ⟨111⟩ or ⟨100⟩). Electron densities calculated from statistical models would predict roughly the same maximum range in both metals. On the other hand, the number of conduction electrons per atom is much smaller in gold than in tungsten, and this might be the reason for the large difference in their observed stopping powers.

Firsov's treatment of electronic stopping and its dependence on impact parameter predicts surprisingly well the approximate magnitude of S_e (Fig. 5) and its general rate of increase with Z_1, particularly considering the nature of the approximations involved. For the ⟨100⟩ channel, a trajectory oscillating by even 0.4 Å from the perfectly channeled case would be enough to raise the Firsov curve to the best mean fit through the experimental points.

Similar (but smaller) oscillations to those in Fig. 5 have been observed in amorphous carbon, aluminum and boron foils by Ormrod *et al.*[25,26,29] and in carbon foils by Fastrup *et al.*[27,28] Presumably these periodic oscillations are related to the shell structure of the penetrating ions, but no obvious correlation can be seen. For example, Na[24] is located at a minimum and

[25] J. H. Ormrod and H. E. Duckworth, Can. J. Phys. **41**, 1424 (1963).
[26] J. H. Ormrod, J. R. Macdonald, and H. E. Duckworth, Can. J. Phys. **43**, 275 (1965).
[27] B. Fastrup, P. Hvelplund, and C. A. Sautter, Kgl. Danske Videnskab. Selskab, Mat.-Fys. Medd. **35**, No. 10 (1966).
[28] B. Fastrup and P. Hvelplund (private communication).
[29] J. R. Macdonald, J. H. Ormrod, and H. E. Duckworth, Z. Naturforsch. **21a**, 130 (1966).
[30] J. Lindhard, Kgl. Danske Videnskab. Selskab, Mat.-Fys. Medd. **34**, No. 14 (1965).
[31] H. E. Schiøtt, (private communication).
[32] F. Brown, G. C. Ball, D. A. Channing, L. M. Howe, J. P. S. Pringle, and J. L. Whitton, Nucl. Instr. Methods **38**, 249 (1965).

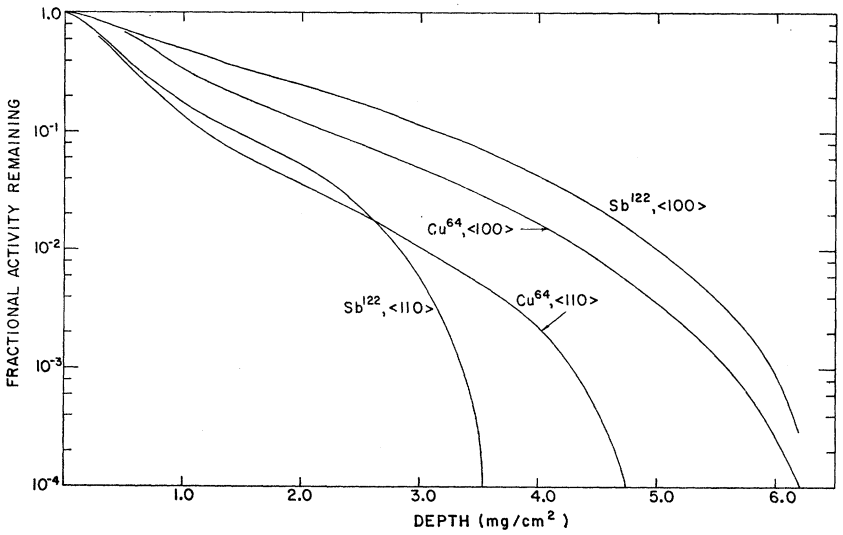

FIG. 8. Integral range distributions of 500-keV Cu^{64} and Sb^{122} ions along the ⟨100⟩ and ⟨110⟩ directions in tungsten.

K^{42} at a maximum. For channeled atoms, the observed oscillations (Fig. 5) are much more pronounced than in the amorphous case, suggesting that these shell effects become more important for collisions at large impact parameters.

So far, a satisfactory explanation of the oscillating Z_1 behavior has not appeared. Such oscillations are not predicted by either of the above-mentioned theoretical calculations, since both are based on the Thomas-Fermi model of the atom.

The S_e curves for the ⟨100⟩ and ⟨110⟩ directions (Fig. 5) appear rather similar. However, Fig. 7 illustrates that, even for the same projectile, the R_{max} values in various crystal directions are not correlated in a simple way to the midchannel values of $\bar{\rho}$. Again, an oscillatory Z_1 behavior is seen, but more experimental points would have been desirable.

The relative difference in R_{max} between the ⟨100⟩ and ⟨110⟩ directions fluctuates from 8% in the case of Cr to 42% in the case of Sb. Projectiles having small S_e values usually exhibit a large relative difference in R_{max}, and vice versa. (This oscillatory behavior is *not* due to the oscillating value of the normalization factor $R_{max}^{\langle 100\rangle}$—in fact, if $R_{max}^{\langle 100\rangle} - R_{max}^{\langle 110\rangle}$ is plotted without normalizing, the Z_1 fluctuations are even larger). Again, the theoretical treatments predict reasonably well the approximate magnitude of the range difference, but not the Z_1 oscillations. These large variations in the R_{max} dispersion for different elements are evident from Fig. 8, in which range distributions for Cu^{64} and Sb^{122} ions at 500 keV are compared. It will be seen that Sb has a slightly larger range than Cu along the ⟨100⟩ and yet along the ⟨110⟩ the order is reversed.

TABLE V. Total and partial stopping cross sections[a] for perfectly channeled Xe^{133} ions along the ⟨100⟩ direction in tungsten.

E(keV)	Measured total stopping S	Extrapolated electronic stopping S_e	Derived nuclear stopping S_n
0.5	3.2±0.4	0.24±0.01	3.0±0.4
1	2.3±0.3	0.34±0.02	2.0±0.3
2	1.6±0.2	0.48±0.03	1.1±0.2
4	1.3±0.1	0.68±0.04	0.6±0.1
8	1.4±0.1	0.97±0.06	0.4±0.1$_5$
12	1.5±0.1	1.18±0.07	0.3±0.1$_5$
16	1.6±0.2	1.37±0.08	0.2±0.2
20	1.8±0.2	1.6 ±0.1	0.2±0.2
32	2.0±0.2	1.9 ±0.1	0.1±0.2

[a] In units of 10^{-14} eV cm²/atom.

2. NUCLEAR STOPPING OF CHANNELED IONS

Although nuclear stopping is very much suppressed for a channeled ion, it still becomes important at lower energies. Experimentally derived nuclear-stopping powers for perfectly channeled Xe ions along the ⟨100⟩ direction (Fig. 3), in the energy range 0.5–32 keV, are given in Table V. These values are obtained by subtracting the extrapolated electronic-stopping contribution from the measured stopping power.

Assuming the momentum approximation to be valid for perfectly channeled ions, one predicts a nuclear-stopping power which (independent of the potential chosen) is inversely proportional to E; this would produce a maximum range proportional to E^2.[33] However, the momentum approximation eventually breaks down at lower energies—because the stopping power must go through a maximum and then decrease as the energy of the particle is spent. Brinkman[34] has given the elastic energy loss in the momentum-approximation region as a function of the parameters in the Born-Mayer potential $V = Ae^{-r/a}$; and Andersen and Sigmund[35] have estimated the energy loss for the lower-energy region where

[33] C. Lehmann and G. Leibfried, J. Appl. Phys. **34**, 2821 (1963).
[34] J. A. Brinkman, J. Appl. Phys. **25**, 961 (1954).
[35] H. H. Andersen and P. Sigmund, Kgl. Danske Videnskab. Selskab, Mat.-Fys. Medd. **34**, No. 15 (1966).

this approximation no longer holds. Erginsoy *et al.*[36] in computer calculations of 1-keV Fe atoms in bcc α iron find the elastic energy loss for channeled atoms to be essentially time-independent down to about 0.1 keV. This implies a stopping power proportional to $E^{-1/2}$.

In order to compare the results in Table V with theory, we first establish whether or not the momentum approximation is valid in our energy region. This is done by comparing the calculated energy transfer in the momentum approximation with the energy transfer predicted by Andersen and Sigmund. If we define E^* as the energy at which maximum transfer occurs, and E_0 as the injection energy, we find (using the potential of Anderson and Sigmund[35]) that E^* is about 70 eV and that the corresponding maximum energy loss is about 30 eV. For very large E_0/E^*, the formulas by Andersen and Sigmund and by Brinkman agree within the expected uncertainty; even at $E_0/E^*=5$ (i.e., at $\sim$0.35 keV), one finds that the momentum approximation predicts an energy loss that is only $\simeq$30% higher than Andersen and Sigmund's value. Hence, throughout our low-energy range ($E>0.5$ keV), the momentum approximation is expected to be a reasonable one.

The best simple power-law fit to the data in Table V is the expression $S_n=K/E^x$ (keV) $\times 10^{-14}$ eV cm^2/atom, where $x=0.85\pm0.1$ and $K=1.8\pm0.3$. The observed value for the energy exponent is rather close to the momentum approximation value of 1.0. However, Erginsoy's value of 0.5 can also be fitted to the *low*-energy data within the estimated errors.

Fitting an equation $S_n=K'/E$ to the data, we obtain $K_{\text{exp}}'=2.1\pm0.4$, which can then be compared directly to that predicted by the momentum approximation. The latter, of course, is very sensitive to the choice of potential:

(i) Using the Born–Mayer potential, which at these large impact parameters (i.e., $\sim$1.5 Å) should be reasonable, and substituting the Born-Mayer constants used by Andersen and Sigmund[37] (viz. $a=0.219$ Å, independent of Z_1 and Z_2, and $A=A_0[Z_1Z_2]^{3/4}$, with $A_0=52$ eV), we obtain $K'=0.62$.

(ii) Using Abrahamson's values of $a=0.27$ Å and $A_0=90$ eV (as quoted by Andersen and Sigmund[37]) we get $K'=5.6$.

The agreement between these Born–Mayer estimates and our experimental value of 2.1 is really quite good, as the predicted stopping power is very sensitive to the choice of a and A. Also, the theoretical estimates are sensitive to the value of the mean impact parameter; due to thermal vibrations, this might differ slightly from the "static" value.

[36] C. Erginsoy, G. H. Vineyard, and A. Shimizu, Phys. Rev. **139**, A118 (1965).

[37] H. H. Andersen and P. Sigmund, Risø Report No. 103 1965 (unpublished).

It should perhaps be pointed out that it will be very difficult to obtain more detailed experimental information about the pure nuclear stopping of a well-channeled atom. At energies greater than a few keV, electronic stopping predominates. On the other hand, at energies less than 1 keV, the range even of a channeled atom becomes comparable to the lattice spacing: for example, for 250-eV Xe^{133} in the $\langle 100\rangle$ direction, removal of 10 Å of tungsten (which is only six atomic layers) left less than 0.08% of the injected activity in the crystal, indicating that in this energy region one has really a "quantized" range distribution—i.e., a significant fraction of the beam becomes stopped within a single atomic layer.

For a perfectly channeled ion, we have seen that nuclear stopping predominates only at very low energies; its contribution to the observed maximum ranges at high energies can therefore be represented by a small constant term. The magnitude of this small correction can be evaluated by a simple integration: For example, for K and Xe at $v=1.5\times10^8$ cm/sec, it corresponds to about 0.7 and 1.5%, respectively, of the maximum range. This correction term, of course, does *not* affect the electronic stopping powers derived in Sec. 1, as it cancels out when the range-energy curve is differentiated.

3. RANGES IN "AMORPHOUS" TUNGSTEN

Previous range measurements in polycrystalline tungsten foils[5] were influenced so much by crystalline effects that even the median range was significantly greater than the theoretically predicted value. To circumvent this difficulty, and subject the Lindhard–Scharff–Schiøtt (LSS) theory[23] to a more careful test, Domeij *et al.*[6] measured ranges in amorphous oxides of aluminum and tungsten at energies up to 160 keV. Recently, similar experiments in Al_2O_3 at this institute[38] have extended the comparison with the LSS theory up to about 1 MeV.

An alternative procedure, however, for obtaining the range in amorphous media is to identify the depth of the first peak in the present single-crystal experiments as the projected range in amorphous tungsten. Particles entering the crystal close to an atomic row are scattered immediately through an angle sufficiently large that they do not become channeled; presumably such particles have a fairly random trajectory, and hence undergo the equivalent of amorphous stopping. Normally, unless the crystal is extremely well aligned, there is an even greater number of particles that are initially channeled but are gradually scattered out of the preferred direction. In many cases, these scattered particles completely distort the "amorphous" peak, and produce an asymmetric one at a depth considerably larger than the amorphous range. However, our experiments show

[38] P. Jespersgaard and J. A. Davies, Can. J. Phys. (to be published).

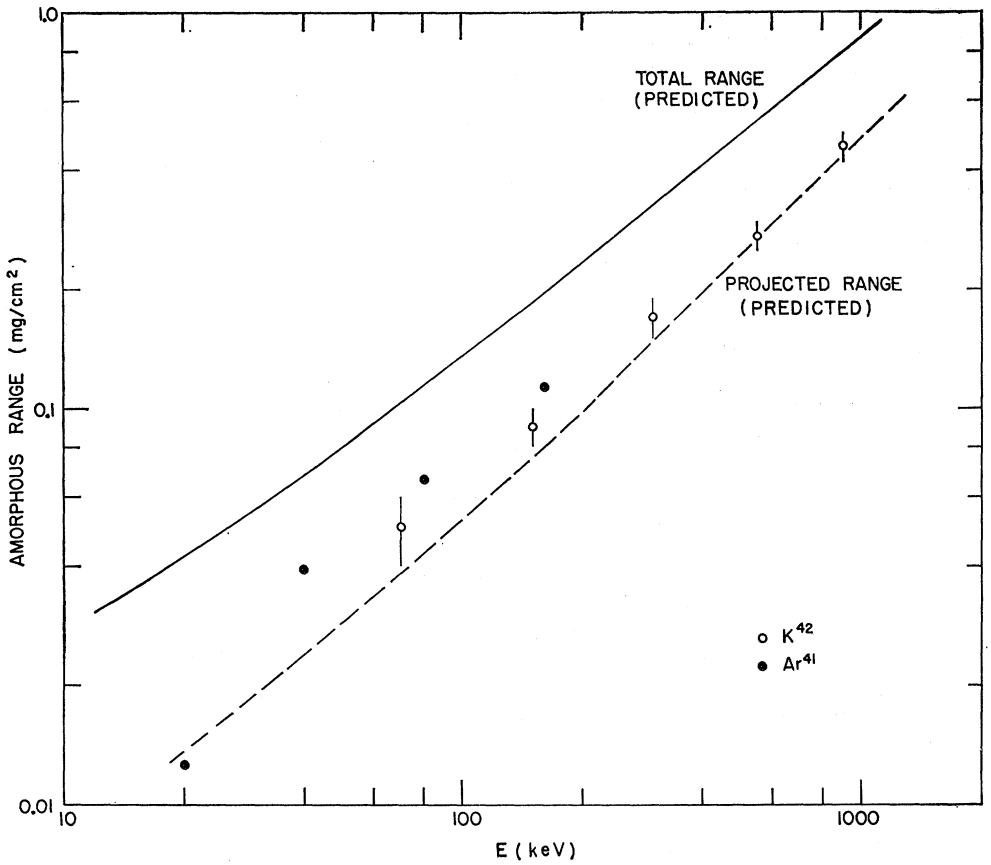

FIG. 9. Projected ranges in "amorphous" tungsten: ○, K^{42} data derived from our measurements in tungsten single crystals; ●, Ar^{41} data obtained from measurements in anodic oxides (Ref. 6). Theoretical curves for the total range (Ref. 23) and for the projected range (Ref. 40) in amorphous tungsten are included.

that there are two ways of obtaining quite reproducible values of the amorphous range from single crystal measurements: (i) by deliberately orienting the crystal to a random direction, so that the channeled *peak* disappears, and nearly all the beam falls into the "amorphous" peak; or (ii) by measuring the range distribution in a preferred direction with very precise orientation, so that the "amorphous" and channeled peaks are both clearly resolved.[39]

To check whether or not method (ii) is applicable to a particular measured distribution, one can roughly estimate (see paper II) that at our energies the "amorphous" peak should contain about 10–15% of the incident beam. If the observed first peak, therefore, contains a higher fraction of particles, it has very likely been distorted by scattering effects from the channeled beam. An illustration of this is given in Fig. 1(b); for the better channeling directions, ⟨100⟩ and ⟨111⟩, the position of the first peak agrees well with the value obtained by random orientation, whereas for the poorer ⟨110⟩ direction, the peak is badly distorted by scattering effects.

Figure 9 shows the projected amorphous ranges obtained for 70–900-keV K^{42} ions. Within the experimental errors, the data agree satisfactorily with the Ar^{41} values of Domeij *et al.*[6] in the overlapping energy region. The solid line gives the total range for K^{42} according to the LSS theory, and the dotted line is the corresponding projected range along the original beam direction. Computer programs that are now available[40] enable the conversion between total and projected ranges to be made accurately even when the projectile is much lighter than the target atom. The agreement with theory is most encouraging.

[39] In principle, the "amorphous" peak in a single crystal should not agree exactly with that in a random stopping medium. When the incident beam is aligned to a main direction, the particles contributing to the "amorphous" peak have all been deflected significantly from the incident direction; hence the *projected* range along the incident direction is somewhat smaller than in a truly amorphous medium. It can be shown, however, that this decrease in our projected ranges is less than a few percent; the correction, therefore, is considerably smaller than the experimental uncertainty.

[40] H. E. Schiøtt, Institute of Physics, University of Aarhus, Denmark, Report, 1967 (unpublished).

In the case of Xe, our measurements, though not so accurate, again agree well with the values predicted by the LSS theory; they also fit smoothly with the lower-energy data[6] (see also Fig. 7, Ref. 10). The measurements give the following projected amorphous ranges:

160 keV: 0.04 ± 0.01 mg/cm^2,

500 keV: 0.10 ± 0.03 mg/cm^2,

1500 keV: 0.28 ± 0.05 mg/cm^2.

It has not been the purpose of this work to investigate amorphous ranges in detail. In fact, the random orientation method (which is the more reliable one) was used only in three runs: viz. for K^{42} ions at 70, 150, and 550 keV.

4. NOTE ON THE SUPERTAIL

Earlier, the supertail phenomenon has been reported in tungsten for Na, Ar, Kr, Rb, Xe, and Cs ions. In addition to these elements we have now observed such tails also for K and Cr ions [see, for example, Fig. 1(a)]. For P, Cu, Br, and Sb ions, it was not possible in the present work to follow the activity to low enough levels to establish whether or not a tail exists. For Rn, on the other hand, Domeij[41] finds no supertail in tungsten, thus supporting Andersen and Sigmund's prediction[42] that even a perfectly channeled atom, if it is heavier than the target atom, will produce appreciable radiation damage near the end of its track, and so presumably will be prevented from participating in the interstitial diffusion mechanism.[15] In order to confirm Domeij's observation, we have carried out a Rn^{222} run at 100 keV in a well-aligned ⟨100⟩ direction. Down to the 5×10^{-6} level, there was no indication of a supertail, even though the fall-off towards a maximum range was very rapid in the last three decades.

Two range distributions have also been measured for 50-keV W^{187} ions along the ⟨100⟩ directions. The activity was followed down to $\sim5\times10^{-5}$ of the original activity, but again no supertail could be observed. This would suggest that the mechanism proposed by Andersen and Sigmund is effective also in the limiting case $Z_1=Z_2$. However, in this "self-diffusion" case, an alternative explanation for the absence of a tail might be the existence of interstitial*cy* diffusion—in which the interstitial moves by a replacement mechanism involving exchange with lattice atoms.

Our measurements at higher energies (where a larger fraction of the beam is channeled) support the earlier conclusion[15] that the supertail typically contains 0.1–1% of the *channeled* particles; they also show that the level of the supertail can easily be reduced by an order of magnitude by slight maltreatment of the crystal.

Five consecutive runs were performed in the same ⟨100⟩ W crystal with 500-keV K^{42} ions. In four of these runs, $0.4\pm0.1\%$ of the *channeled* particles appeared in the supertail; in the fifth run, the corresponding value was less than 0.02% (in fact, only a slight tendency towards a supertail behavior could be observed). However, in this fifth run, the crystal had been deliberately prebombarded with stable K^{39} ions to a total dose of about 10^{15} atoms/cm^2. This sensitivity of the tail to ion bombardment is perhaps not surprising, since a concentration of trapping centres of even 10^{17}/cm^3 should significantly affect both the level and the slope of the supertail.[15] The above prebombardment dose, penetrating to a depth of approximately 1μ, produces a potassium atom concentration in excess of 10^{19}/cm^3 in the region where the channeled radiotracer atoms come to rest.

5. RANGES IN MONOCRYSTALLINE ALUMINUM

For comparison, a few range measurements have also been performed in the ⟨110⟩ and ⟨100⟩ directions of monocrystalline aluminum, using Na, K, and Xe ions at energies up to 500 keV.

The data presented in this section were obtained using only the x-ray alignment technique (i.e., $\pm1°$).

Previous studies on Al,[8] W,[10] and Si [12] showed that the thickness of metal removed by the anodizing-stripping technique is essentially independent of the crystallographic orientation of the target surface. However, for Al crystals, Selig *et al.*[43] have recently reported about a 15% difference in weight loss between {110} and {100} surfaces at an anodizing voltage of 100 V. We have therefore carried out a careful calibration check to establish whether or not the voltage-thickness relationship for Al is truly independent of the orientation. Our technique consisted in measuring the transmission of 400-keV Kr^{85} through Al_2O_3 layers grown at fixed voltage on the {110}, {100}, and {111} surfaces of monocrystalline Al; a similar study has recently been made at Chalk River[44] using 60-keV Na^{24}. In both sets of experiments, the fractional transmission did not depend significantly on the nature of the underlying surface. Comparison with the recently measured range distributions in amorphous oxides[6,38] confirmed that any orientation dependence of the voltage-thickness calibration is less than 1%. This conclusion does not agree with Selig *et al.*'s measurement,[43] and suggests that the effective surface areas of their two crystal faces were significantly different, due perhaps to fluctuations in the surface "roughness" factor.

For several reasons, these range measurements in Al have not been carried out in nearly as much detail

[41] B. Domeij, Arkiv Fysik **32**, 179 (1966).
[42] H. H. Andersen and P. Sigmund, Nucl. Instr. Methods **38**, 238 (1965).
[43] O. Selig and R. Sizmann, Nukleonik **8**, 303 (1966).
[44] J. L. Whitton and G. Sims (private communication).

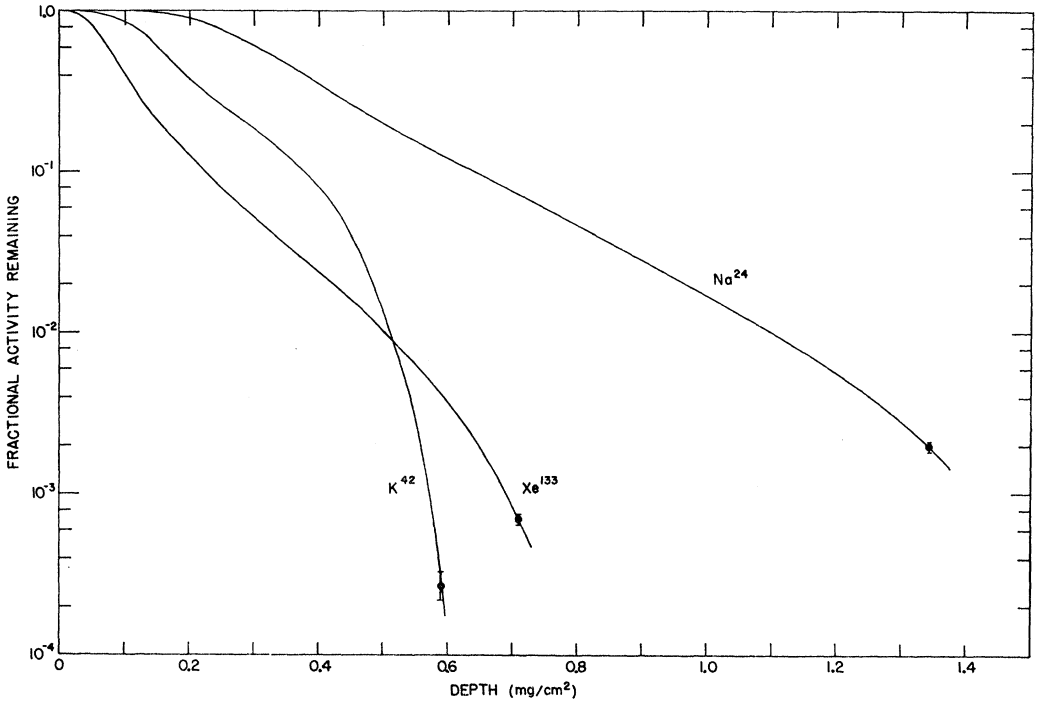

FIG. 10. Integral range distributions of 500-keV Na^{24}, K^{42}, and Xe^{133} ions along the ⟨110⟩ directions in aluminum.

as those in W. Firstly, the channeling in aluminum, even in the best direction (i.e., ⟨110⟩), is poor compared to that in tungsten. This was already evident in the lower-energy work by Piercy *et al.*[8] Secondly, the anodizing-stripping technique[45] for aluminum is much more time consuming and somewhat less accurate than for tungsten.

TABLE VI. Values of $R_{10^{-3}}$ in monocrystalline aluminum.

Ion	E(keV)	$R_{10^{-3}}$ (mg/cm²) ⟨110⟩	⟨100⟩
Na^{24}	40	0.27[a]	~0.20[a]
	80	(0.5)	0.37
	200	0.64	(0.45)
	300	0.80	•••
	500	(1.45)	(0.9)
K^{42}	150	0.28	0.25
	500	0.57	0.52
Kr^{85}	20–160	See Ref. 8[b]	
Xe^{133}	40	0.09[a]	0.06[a]
	140	0.32	0.22
	500	0.69	0.53

[a] From Ref. 8.
[b] See Ref. 8.

[45] J. A. Davies, J. D. McIntyre, R. L. Cushing, and M. Lounsbury, Can. J. Chem. **38**, 1535 (1960).

Figure 10 shows integral range curves for 500-keV Na, K, and Xe ions injected along the ⟨110⟩ directions. It is quite obvious that in aluminum we cannot estimate the true maximum range unless the range distributions are followed to much lower levels. Only the potassium curve approaches a maximum range at the 10^{-3}–10^{-4} level, which is the typical lower limit of our measurements. However, even this curve, when differentiated, does not produce a double-peaked distribution. The almost exponential decrease observed for Na and Xe indicates that scattering of the channeled beam out of the aligned direction is much more pronounced in aluminum. Even in the favorable case of 500-keV K^{42} in the ⟨110⟩ direction, only a few percent of the particles remain channeled throughout most of their range. This is to be compared with more than 75% for the favorable ⟨111⟩ direction in tungsten. The difference in channeling magnitude cannot be attributed entirely to the much thicker surface oxide on aluminum, because range measurements in gold at room temperature[46] exhibit a similar exponential decrease in spite of the oxide-free surface. Presumably, in both Al and Au, the much larger vibrational amplitudes of the lattice atoms at room temperature are part of the explanation.

Table VI summarizes the experimental results. We have somewhat arbitrarily selected the 10^{-3} level for this comparison; these values are quite sensitive to

[46] J. L. Whitton, Can. J. Phys. **45**, 1947 (1967).

TABLE VII. Electronic stopping cross sections S_e and range dispersions in aluminum at $v=0.9\times10^8$ cm/sec.

Ion	E(keV)	S_e[a] Experimental ⟨110⟩	⟨100⟩	S_e[a] Lindhard (amorphous)	S_e[a] Firsov ⟨110⟩	Range dispersion[b] $(R\langle110\rangle-R\langle100\rangle)/R\langle110\rangle$
Na^{24}	101	2.0	2.8	4.9	2.0	27%
K^{42}	176	4.1	5.0	7.0	2.4	11%
Kr^{85}	357	7.1[b]	...	10.0	3.1	~20%[c]
Xe^{133}	558	7.0	9.0	12.0	3.8	22%

[a] In units of 10^{-14} eV cm²/atom.
[b] R values measured at the 10^{-3} level.
[c] Extrapolated from Ref. 8.

misalignment, etc., particularly in the case of Na and Xe—and hence the tabulated values are not too reproducible. The $R_{10^{-3}}$ values, plotted against energy, approach an $E^{1/2}$ dependence as was observed in tungsten, but the accuracy is not as high. Hence, once again, electronic stopping is the dominant mechanism of energy loss for channeled heavy ions even at fairly low energies. A similar conclusion was reported earlier[8] from range studies of Kr^{85} in aluminum at energies up to 160 keV.

Table VII contains the electronic-stopping powers for the ⟨110⟩ and ⟨100⟩ directions (typical errors ±20%) derived at the constant velocity $v=0.9\times10^8$ cm/sec. This is the velocity used by Ormrod *et al.*[26] For comparison, the *electronic*-stopping powers predicted for amorphous aluminum[23] and for a channeled atom moving in the geometrical centre of the ⟨110⟩ channel[24] are included. The experimental points are too few to establish whether or not an oscillating dependence on Z_1 exists similar to that observed in tungsten (Fig. 5).

It should be noted that, since in aluminum the range measured at the 10^{-3} level is not a good approximation to the maximum range, the derived stopping powers will be too high, particularly in the case of Na, Kr, and Xe.

Table VII also lists the range dispersion between the ⟨110⟩ and ⟨100⟩ directions in aluminum.

In conclusion, monocrystalline aluminum is evidently not a very suitable choice for studying quantitatively the channeling of heavy ions. The general behavior, however, is similar to that observed in monocrystalline tungsten.

ACKNOWLEDGMENTS

We are very grateful to our colleagues—particularly J. Lindhard, J. U. Andersen, B. Domeij, B. Fastrup, E. Kornelsen, K. O. Nielsen, H. E. Schiøtt, and P. Sigmund—for many stimulating discussions throughout this work. We also wish to thank P. Kjaer and J. Thorsager for helping us with the ion bombardments. Two of us (J. A. D. and L. E.) are especially indebted to Professor K. O. Nielsen for the invitation to work in his accelerator group for an extended period. This work was financially supported by the Danish State Research Foundation.